Proc. Natl. Acad. Sci. USA
Vol. 91, pp. 5133–5137, May 1994
Biochemistry

Three-dimensional working model of M1 RNA, the catalytic RNA subunit of ribonuclease P from *Escherichia coli*

(precursor tRNA/computer modeling)

ERIC WESTHOF* AND SIDNEY ALTMAN†

*Institut de Biologie Moléculaire et Cellulaire, Centre National de la Recherche Scientifique, 15 rue René Descartes, 67084 Strasbourg-Cedex, France; and †Department of Biology, Yale University, New Haven, CT 06520

Contributed by Sidney Altman, February 14, 1994

ABSTRACT **A three-dimensional model of M1 RNA, the catalytic RNA subunit of RNase P from *Escherichia coli*, was constructed with the aid of a computer. The modeling process took into account data from chemical and enzymatic protection experiments, phylogenetic analysis, studies of the activities of mutants, and the kinetics of reactions catalyzed by the binding of substrate to M1 RNA. The model provides a plausible picture of the binding to M1 RNA of the tRNA domain of a precursor tRNA substrate. The scissile bond and adjacent segments of the aminoacyl acceptor stem of a precursor tRNA substrate can fit into a cleft that leads to the phylogenetically conserved, central part of the structure.**

Computer-assisted modeling has been of particular value in providing some understanding of structure–function relationships for large RNA molecules with well-defined biological roles (1–6). This approach to the understanding of the structural features of RNAs is especially important in cases where a large amount of biochemical and genetic data already exists with respect to structure–function relationships but a crystallographic definition of a particular structure is unavailable. Although such models do not allow us to make statements about molecules with the same degree of confidence as when their structures are derived from crystallographic information, they can point the way to explicit analysis of detailed structural features and structure–function relationships. Such models serve, therefore, as working tools and are not intended to be taken as final definitions of particular structures. Nevertheless, if a model is compatible with a sufficiently large body of noncrystallographic data from studies of structure and of structure–function relationships, we can infer that the model has merit.

We present here a working model for the structure of M1 RNA, the catalytic RNA subunit of RNase P from *Escherichia coli* (7, 8). RNase P is an enzyme that contains a catalytic RNA subunit 377 nt long (M1 RNA) and a protein subunit of about 14 kDa (C5 protein). This endoribonuclease is responsible for the creation of the 5′ termini of all mature tRNAs from their precursor molecules. It represents a paradigm for the study of catalysis by RNA and for RNA–RNA and RNA–protein interactions. Our model, which is compatible with results of a variety of studies on RNase P, leads to several predictions that provide a basis for further work and therefore should be regarded as a step towards the definition of a three-dimensional structure for the enzyme.

MATERIALS AND METHODS

Molecular modeling was performed for the most part as described (6). Using in-house programs and starting with the primary sequence of M1 RNA, we constructed stem–loop structures and other elements of secondary structure found in the general model of the secondary structure of M1 RNA and its analogs (9) in the order in which they are numbered in Figs. 1 and 2. Subsequently, these structural elements were assembled into a three-dimensional structure by using a computer graphics station and FRODO (12) software. The general model was geometrically refined with the NUCLIN-NUCLSQ program (13). The latter program varies the positions of 8107 atoms found in the 377 nt of M1 RNA in a fashion that guarantees the absence of bad contacts while maintaining correct geometry. Appropriate stereochemistry is incorporated in the model under the constraints imposed (*i*) by hydrogen-bonding contacts derived from the earlier two-dimensional structure that was based on phylogenetic analysis (9), (*ii*) by potential pseudo-knotted regions (9, 14, 15), and (*iii*) by additional tertiary base pairs revealed during the modeling process. During such a stratified approach to modeling, uncertainties are present at every level, and both the origin and the propagation of errors (including the identification of the weakest link in the process) are difficult to assess. Nevertheless, the usefulness of such a modeling process resides not in its current level of precision but in the predictive power of the process itself and of the end product.

RESULTS

M1 RNA. The three-dimensional model of M1 RNA is shown in Fig. 2. The various helical regions are represented by different colors to emphasize their paths in space. For clarity, the molecule is shown as a collection of ribbon-like segments. Stem–loop structures and other hydrogen-bonded interactions found in the general model of secondary structure (8, 9) were constructed (Fig. 1) as indicated in *Materials and Methods*. At this early stage of construction, the model of the structure of M1 RNA was partially constrained in three dimensions by the pseudo-knot that creates P12 (paired, double-stranded helix; see Fig. 1) and the proposed hydrogen-bonding of nt 82–85 with nt 276–279 (P13; ref. 14), but otherwise many degrees of freedom remained possible for some of the subdomains of the enzyme. Recent data (15) that indicate the existence of additional long-range, hydrogen-bonded base pairs (120–237 and 121–236) have also been included. The modeling process itself, as well as phylogenetic data, also suggested that nt G127·U231, C128·G230, and A129·G229 (P14) might constitute another set of base pairs: these base pairs aid in the appropriate orientation of P5–P6. The results of intramolecular UV cross-linking experiments, in which C122 is cross-linked to U231, are also compatible with the existence of P14 (C. Guerrier-Takada and S.A., unpublished data) as are studies of mammalian analogs of M1 RNA (16).

The publication costs of this article were defrayed in part by page charge payment. This article must therefore be hereby marked "*advertisement*" in accordance with 18 U.S.C. §1734 solely to indicate this fact.

Abbreviations: ptRNA, precursor tRNA; E–S complex, enzyme–substrate complex.

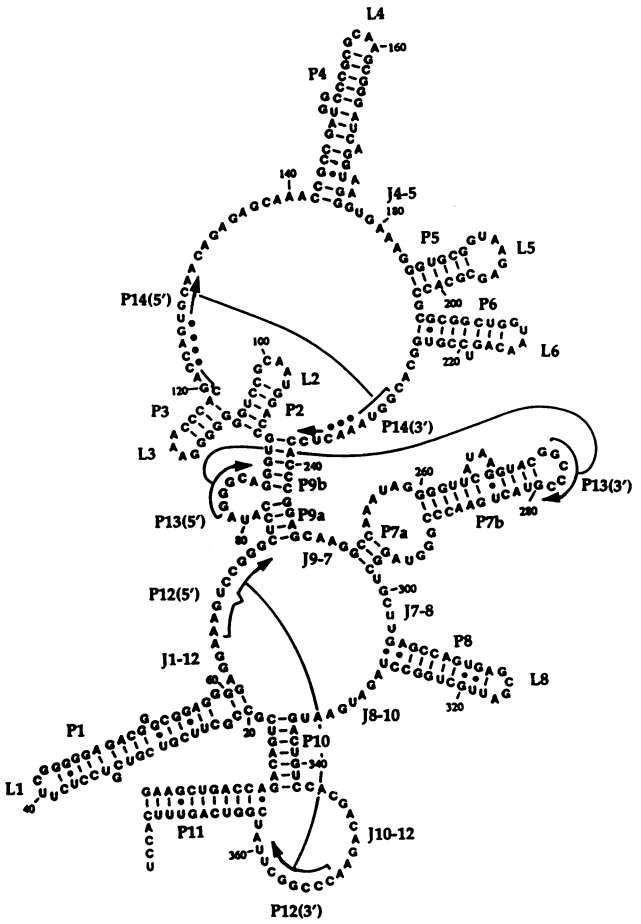

FIG. 1. Sketch of the proposed two-dimensional structure of M1 RNA based on the model in ref. 8, showing the nomenclature employed herein and long-range interactions incorporated into the three-dimensional model. The nomenclature of the elements of secondary structure follows that used for group I introns (10): P indicates paired, double-stranded helices (when interrupted by a bulge or an internal loop, lowercase letters are added to the number that designates the helical segment—e.g., P9a); L indicates hairpin loops; and J indicates junction segments connecting two double-stranded helices (e.g., J4–5 connects P4 to P5). The black dots in P14 indicate uncertainty as to the extent and nature of hydrogen-bonded base pairs in this part of the helix.

Inspection of the two-dimensional model indicated that certain helices might be stacked on others (e.g., P1 stacks on P10, which stacks on P11, and P5 stacks on P6), and these possibilities were initially incorporated into the model and later refined. Furthermore, the appearance of the sequence GNRA (where R = G or A and N = G, A, T, or C) in the loops of certain helices (P3, P4, P6, and P8) suggested, on the basis of the modeling of other RNAs (3, 17), that these loops might be important in establishing long-range interactions either between various regions of M1 RNA or between M1 RNA and a precursor tRNA substrate. Additionally, chemical protection data (18) support the existence of an interaction between L6 (hairpin loop 6; see Fig. 1) and the middle base pair of the second segment of P9 (P9b). This contact allowed us to finalize the position of the subdomain P5–P6 and led to the appearance of a potential contact between L2 and the middle base pair of P5. The temperature-sensitive phenotype of the mutant G200 (19) led us to retain the latter contact. Finally, an examination of many sequences of the procaryotic analogs of M1 RNA (8, 9) led to the conclusion that the model we present here can be generalized. When contacts proposed in the model of M1 RNA are absent from some analogs of this molecule, equivalent contacts can often be made by using structural elements present in those analogs and missing from M1 RNA.

We postulated that one indication of the success of our model would be the appearance of a cleft or pocket into which a substrate [precursor tRNA (ptRNA)] could fit: such a cleft was readily apparent in the model shown in Fig. 2, even prior to any refinement. The model was further refined by reference to data from various chemical modification experiments in which the accessibility of bases (refs. 18 and 20; S.A., unpublished experiments) was probed and is in general agreement with the results of experiments on the binding of complementary oligonucleotides to different regions of M1 RNA (21).

The Enzyme-Substrate (E–S) Complex. Orientation of the substrate on the enzyme was attempted with a standard tRNA with known structural coordinates, yeast $tRNA^{Asp}$ (13), as a substitute for an actual substrate since our initial presumption was that the highly variable precursor-specific sequence of true substrates would be single-stranded and very flexible, whereas the tRNA domain would not be flexible and therefore would impose greater constraints on the modeling process. Chemical protection data for M1 RNA in E–S complexes also indicated those nucleotides in M1 RNA that should be protected in the presence of a substrate (20). Taking these factors into consideration, we found that the tRNA domain in a substrate is oriented in a pocket in the structure of M1 RNA so that it is flanked by P4 and P8 as shown in Fig. 3. In this figure the details of the atomic contacts between the enzyme and the substrate are left unspecified because this simplifies the view of the model and because those details can only be rigorously determined by crystallographic studies. The site to be cleaved, adjacent to nt +1 at the 5′ terminus of the acceptor stem, lies deep in the pocket close to the central part of the folded structure of M1 RNA (see below). Similar success in positioning a tRNA with a long, variable loop ($tRNA^{Ser}$), the atomic coordinates of which are also known (22), was also achieved. Further useful and detailed information about possible placement of a substrate came from cross-linking experiments.

A ptRNA and a tRNA with a photoactivated cross-linking agent attached to it at various positions have been cross-linked to M1 RNA (23–25). In general, the data from such experiments are also compatible with our model in which the placement of nt +1 in the tRNA domain of a substrate is close to nt 249 and 330 of M1 RNA. The latter two nucleotides are close to each other, as determined with a photoactivated agent with an effective radius of interaction of at least 9 Å (24, 25). The scissile bond lies principally between two regions centered on residues A248 and C353. (In the present model, C353 forms a trans Watson–Crick base pair with G74 and a triple base interaction is also possible with C247.) The J8–10 function portion (centered on position 330) is nearby and extends "below" these two regions. A critical interaction in our model occurs with the base pair G53·C61 in the tRNA. This base pair is highly conserved (42) in all elongator tRNAs (see below).

One poorly understood aspect of the action of RNase P is the manner in which the enzyme chooses its cleavage site with such accuracy. Our model indicates that the acceptor stem (or its equivalent in model substrates) is the portion of a substrate that forms the most intimate contacts with the hypothetical catalytic center of the enzyme, a region that we estimate includes J9–7 (CAAG) and the 3′ end of J10–12, J8–10 (AGAU), and the 3′ side of the bulge of P7 (GGUA; see below). If a measuring device for identification of the site of cleavage in each substrate exists in the enzyme, then the distance measured from the top of the acceptor stem (or its continuation, the T stem) to the site of cleavage on the 5′ side of nt +1 in the acceptor stem in ptRNAs is likely to be critical. Accordingly, the interactions with P3, and in particular with

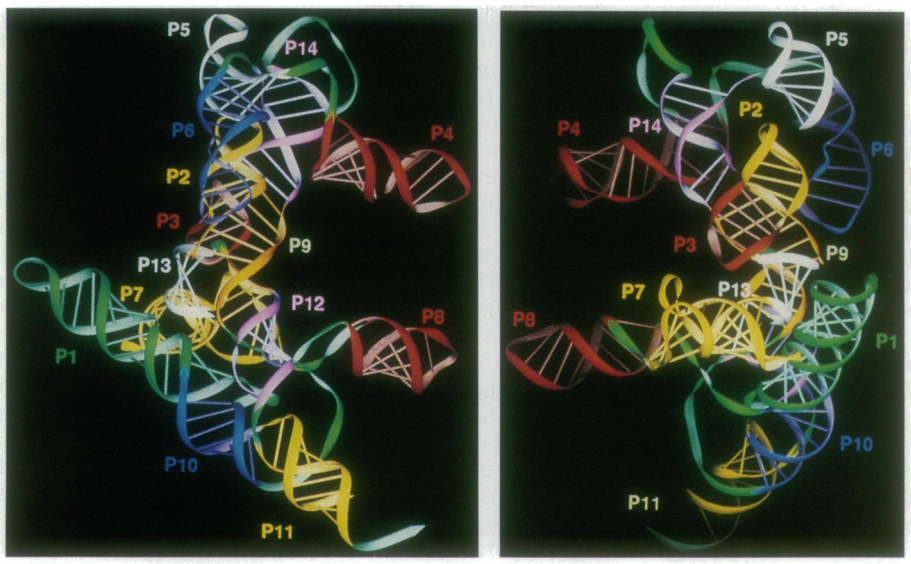

FIG. 2. Views of the three-dimensional model of M1 RNA. The left and right views differ from each other in terms of rotation by 135° around the vertical axis. The different helices are numbered and are represented in various colors. The numbers are in the same colors as the helices that they designate. Except for P1, only the single-stranded regions are in green. Arrows in ribbons point to the 3′ end of the phosphodiester chain. The representations were produced with DRAWNA software (11).

its terminal loop that contains GNRA (found in all analogs of M1 RNA in procaryotes), are likely to be important. In addition, since the G53·C61 base pair at the "top" of the T stem in tRNA is almost always found in all tRNAs (ref. 42; excluding some unusual tRNAs in subcellular organelles), the model was finalized by determining whether the GNRA loop of P3 (L3) or that of P4 (L4) might serve as an anchor for the tip of the T stem. The positioning of P3 with respect to P2–P9 is, itself, dictated by the proposed pairings in P14 (15) and the contact made by the P5–P6 subdomain with the P2–P9 subdomain. Additionally, it has been shown (25) that G53 of the G53·C61 base pair in tRNA can be cross-linked to L3, thus verifying another contact (G53 in tRNA with A114 in M1 RNA) that is predicted by our model. P3 and P4 have been strongly implicated in contacts with the substrate in the chemical experiments (20), and such contacts with the T stem and loop are obvious, as shown above. Although P4 and L4 interact with the anticodon stem, the anticodon stem and loop play a relatively minor role in the precise positioning of the tRNA on the enzyme, as expected from an examination of other non-tRNA precursor substrates (refs. 26 and 27; H. Inokuchi, personal communication) and "*in vitro* evolution" experiments (28).

Depending on the state of denaturation of the acceptor stem, the 3′-terminal CCA sequence of the tRNA domain can be placed in different positions. In this regard, chemical and enzymatic protection experiments with E–S complexes have shown that the acceptor stem in the tRNA domain is partially denatured (refs. 20 and 29; R. K. Gaur and G. Krupp, personal communication) and that the secondary pairings of that domain are disrupted after initial binding to the enzyme has been achieved (20). These observations are also consistent with physical studies that show that denaturation of the tRNA domain facilitates binding of both certain substrates and mature tRNA to the enzyme (21). Such a denaturation of the substrate [the terminal base pair of the aminoacyl acceptor stem is also denatured in the binding of $tRNA^{Gln}$ to its cognate synthetase (30)] allows placement of both the 5′ and 3′ strands of the acceptor stem that is closely compatible with the results of the studies of E–S complexes cited above while maintaining the position of the rest of the tRNA domain. Therefore, the acceptor stem is almost completely denatured in our model. Furthermore, recent genetic experiments (L. Kirsebom, personal communication) have indicated that A73-C74 of the tRNA domain very likely form base pairs with U294-G293 in M1 RNA during catalysis. To establish such contacts in our model, the acceptor stem must be partially denatured. If the stem is not denatured, the CCA sequence interacts with the G63-G64 region or the shallow groove of P12 in M1 RNA. Site specific mutagenesis experiments (C. Guerrier-Takada, R. Meng, and S.A., unpublished data) show that the region around G63 in M1 RNA must be intact for catalysis to occur and is important for local folding but not for interactions with the CCA sequence. The proposed contacts in the internal bulge of P7 are also compatible with the positions of cross-links made to M1 RNA by tRNA with a

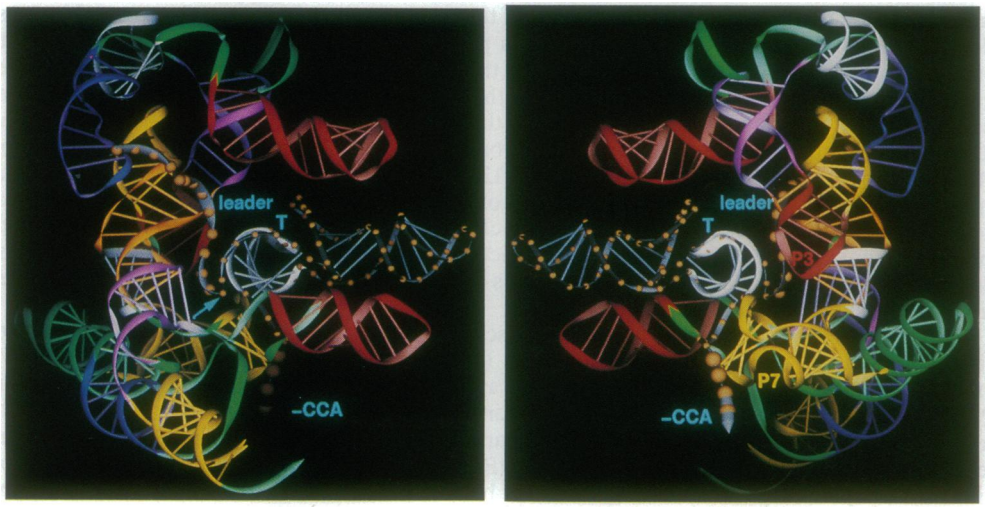

FIG. 3. Views of the three-dimensional model of the complex of M1 RNA and a tRNA precursor molecule (see text). The orientations and the color code for M1 RNA are the same as those shown in Fig. 2. The ptRNA molecule is silver (except for the T loop of the tRNA domain, which is white), and its phosphorous atoms are embedded in brown spheres. The sizes of the spheres indicate different regions of the ptRNA: smallest spheres, tRNA domain; intermediate-size spheres, 5′ leader sequence; and largest spheres, 3′ CCA sequence. (*Left*) The site of cleavage is indicated by an arrow.

photoactivatable cross-linker attached to its 3′ terminus (B.-K. Oh and N. R. Pace, personal communication).

tRNA molecules with a photoactivated cross-linker attached at G53 of the tRNA make a cross-link with L3 as indicated above (25) but also react with other sites near C348 in M1 RNA. Similarly, if the cross-linking agent is attached to G64 of the tRNA, several sites in M1 RNA are found to be reactive. Some of these cross-links are compatible with our model (i.e., G53 to L3, A64 to P9a, J9/7), whereas others are not (i.e., G53 to J10/12, G64 to J1/12) unless the tRNA is rotated by 180° on the surface of the enzyme, in which case the regions in M1 RNA mentioned above come into contact with the appropriate positions in the tRNA. The cross-link observed between C92 in M1 RNA and cytosine at position −3 in pTyr (23) is consistent with the first mode of binding of the substrate to the enzyme if the cross-link is made prior to the formation of a complex that can assume the conformation of the transition state. We regard these results as indicative of the existence of more than one binding site of ptRNA and tRNA on M1 RNA, as we inferred in previous kinetic studies of the enzymatic reaction (21) and from direct cross-linking studies with UV light (23). These modes of binding do not compete directly with each other, since only one (the first described above) would lead to catalytic cleavage by the enzyme of a ptRNA. The cross-linking studies also provided evidence for another mode of binding to M1 RNA (that facilitates cross-links between G64 and position 118 and L2 in M1 RNA) that is clearly incompatible with our model in the sense that the site to be cleaved in a ptRNA is distant from the active center: this last site is artifactual or clearly noncompetitive in terms of the cleavage reaction. Clearly, the E–S structure probed in chemical or cross-linking experiments cannot be stated unequivocally to represent a single stable configuration of a catalytically active E–S complex, since the result of a cross-linking experiment is a picture frozen in time of ligands entering, already in, or leaving binding sites on the enzyme.

The ptRNA-like structure found in turnip yellow mosaic virus (TYMV) is cleaved by RNase P at the end of one of the two helices that form the pseudo-knot at the 3′ end of the viral RNA (26), while that of brome mosaic virus (BMV) is not. An attempt was made to orient both of these molecules, which have been modeled by computer (31, 32), on our model of M1 RNA in positions similar to that of a ptRNA: the TYMV structure could be appropriately positioned on the assumption that L3 of M1 RNA interacts with a purine "below" the TYC-like loop (where Y = T or C) of TYMV. The BMV structure could not be positioned in the same way because it has bulky appendages.

DISCUSSION

We have constructed a three-dimensional model of M1 RNA using computer-assisted methods. Our model allows us to visualize the placement of a substrate on the surface of the catalytic RNA and to suggest the location and features of the catalytic center. However, we recognize that it is difficult to define rigorously the entire M1 RNA molecule because of its sheer size. Furthermore, since M1 RNA functions *in vivo* as part of a ribonucleoprotein complex, comparisons between the sequence of this molecule and its analogs are not always useful in a straightforward fashion for attempts at modeling. Covariations of pairs of nucleotides in the sequences could be due to the need to maintain protein–nucleic acid contacts and the higher-order structure in M1 RNA itself. However, our model is consistent with a large body of empirical data, and many of its features allow us to make hypotheses about the mechanism of action of RNase P and the effects on function of mutations in the substrate and the enzyme.

The model provides a glimpse at a mechanism for RNA enzyme–RNA substrate interactions for enzymes that have many substrates with a variety of primary sequences: recognition is not governed by a linear series of Watson–Crick hydrogen bonds between sequences in the enzyme and substrate. Instead, a diversity of interactions (van der Waals docking, hydrogen bonding to ribose hydroxyl groups, base "triple" interactions in the shallow groove, and bridges mediated by hydrated magnesium ions) occurs between a deep and extended pocket of the enzyme and the helical substrate. Autocatalytic introns employ guide sequences to form first the helical substrate that will then dock and be recognized by a similar set of interactions to those mentioned above (33). As it stands, the model incorporates several RNA–RNA contacts within M1 RNA and some between M1 RNA and the ptRNA substrate that are compatible with most of the sequences of M1 RNA and its analogs that are now available. Since the holoenzyme is a ribonucleoprotein, one can expect that some of the RNA–RNA contacts that we have suggested in our model might be replaced by RNA–protein interactions. The presence of the C5 protein cofactor clearly adjusts the structure of M1 RNA so that cleavage by the holoenzyme of certain substrates occurs at the correct or expected site, whereas cleavage by M1 RNA alone of these substrates occurs at unexpected sites (23).

The testable structural features of our model that are not apparent from previous studies are as follows: GNRA of L6 interacts with the shallow-groove side of the base pair G89·C240 in P9b. The adenine residues of L2 interact with the shallow-groove side of P5 close to the base pair U186·A200. Since J3–4 and J6–9 are in close proximity, previously unidentified interactions, which remain to be defined precisely, must exist between these two regions other than those recently identified (15). The active site (see below) is in the region of J9–7, the 3′ end of J10–12, and part of J8–10. The accurate positioning of the tRNA domain of a substrate on M1 RNA occurs through the interaction of GNRA in L3 with base pair G53·C61 at the base of the T stem in the tRNA. The adenine residues of the 5′ segment of the internal bulge in P7 might interact additionally with the *O*-2′ hydroxyl groups in the shallow groove of the T stem of the ptRNA substrate. The anticodon arm of the tRNA is sandwiched between P4 and P8, while the acceptor stem is denatured, the 5′ strand is buttressed against J9–7, and the first two bases of the 3′-terminal GCCA sequence interact with the 3′ side of the internal bulge of P7. In fact, the general features of the model of the enzyme, the E–S complex, and a complex of the enzyme with its protein cofactor are compatible with experiments in which the structure of M1 RNA has been probed under various conditions with an Fe(II)–EDTA reagent (S.A., D. Wesolowski, and E.W., unpublished data).

The conservation throughout evolution of the pseudo-knot P12 (9) is striking; therefore, we might reasonably expect it to be part of the catalytic site (similar to P7 in group I introns: this helix is part of a pseudo-knot and forms at one of its extremities the binding site for the guanosine cofactor required for the phosphotransferase reaction). As a consequence of the formation of P12, several single-stranded regions are brought together to form the catalytic site at the 3′ end of P12(5′). However, it is premature to discuss the mechanism of catalysis in great detail because the empirical data on which we have based our model do not allow us to resolve structural details at the atomic level. Nevertheless, two schemes can be proposed, the second of which subsumes the first.

The first scheme is consistent with a proposed mechanism of catalysis (34) that involves one Mg^{2+} ion at the active center: the attacking water molecule (or hydroxide ion) is part of a coordination sphere of an Mg^{2+} ion that is bound to M1 RNA (candidates in the current model could be U331 and C351). The tRNA domain of a ptRNA is pushed against P9 by (*i*) contacts between L3 and G53·C61 in the tRNA, (*ii*) the

adenine residues on the 5′ side of the internal bulge in P7 that bind in the shallow groove of the extended T-acceptor stem, and (*iii*) the 3′-terminal end of the tRNA that interacts with the 3′ side of the internal bulge in P7 and is in a position to form hydrogen-bonded bases pairs. Therefore, a strain is imposed on the 5′ end of the ptRNA leading to a sharp kink at the cleavable phosphate that is positioned on "top" of the bound Mg^{2+} ion mentioned above. This strain, itself, confers lability on the scissile bond.

The second scheme for catalysis involves two Mg^{2+} ions, one on either side of the scissile bond. This scheme has similarities to previously proposed mechanisms of cleavage of phosphoester bond (35–37). In this scheme, one Mg^{2+} ion is bound to the substrate at positions −1 and −2 in the leader sequence. Such a Mg^{2+} ion has been implicated previously in catalysis (38), and it is positioned on one side of the scissile bond close to P9(5′) and J9/7. The second Mg^{2+} ion, positioned on the other side of the scissile bond, might be the one described above in the "single-ion" mechanism. This scheme is attractive because it is compatible both with a large amount of data that implicates both nt −1 and −2 as being important in the mechanism of bond cleavage (35, 38, 39), very likely through the formation of a metal ion-binding site, and with mechanisms in which two divalent metal ions serve as a general tool for facilitating cleavage of phosphoester bonds.

Many mutants of M1 RNA and ptRNA substrates have been characterized (for examples, see refs. 7, 14, 19, 40, and 41). In some cases, these mutations (A89, G200) have been valuable in attempts to define base-pairing interactions between nucleotides, and these interactions were incorporated into the model-building process. In most other cases, the structural consequences of these mutations were unknown or have only been postulated. For example, deletion of A65 results in loss of the activity of M1 RNA: in our model, such a deletion results in a dramatic alteration in the direction of the phosphoester backbone chain near the catalytic center. We have postulated that C247 is at the heart of the active center and might interact with the 5′ terminus of the acceptor stem of a substrate, in particular with nt +1, which is most frequently G. Indeed, substitution of G or A at position 247 results in a reduced rate of cleavage by M1 RNA, whereas substitution of U has no effect (C. Guerrier-Takada, R. Meng, and S.A., unpublished data), as might be expected if the interaction with G1, which is present in most but not all substrates in *E. coli*, is mediated by classical Watson–Crick hydrogen bonding. Similarly, we predict that the internal bulge in P7 might play a role in positioning Mg^{2+} ions that are important for catalysis and/or positioning of the substrate on the enzyme in our model: in fact, deletion or alteration of nt 291–295 not only leads to very reduced levels of catalytic activity but also to cleavage at an inappropriate site in some ptRNAs (ref. 41; L. Kirsebom, personal communication).

It is impossible, at the moment, to state whether or not the three kinds of substrate binding that we have described all actually represent three metastable states of E–S complexes or result from modeling errors. One of the binding modes may indeed correspond to a site of binding of the product (tRNA) and not the substrate (ptRNA), and it may be more important in determining the rate of product release than the kinetics of the chemical step of the reaction. The path of the enzymatic reaction may require the substrate, after it has been converted to the product by the chemical event, to move from one of these bound states to another.

We thank Donna Wesolowski for her excellent technical assistance, C. Guerrier-Takada for many helpful discussions, C. Massire and P. Auffinger for the preparation of color illustrations, and colleagues for communicating results prior to publication. Research in the laboratory of S.A. is supported by Grant GM19422 from the U.S. Public Health Service and research in the laboratory of E.W. is supported by the Centre National de la Recherche Scientifique.

1. Westhof, E., Romby, P., Romaniuk, P. J., Ebel, J.-P., Ehresmann, C. & Ehresmann, B. (1989) *J. Mol. Biol.* **207**, 417–431.
2. Brunel, C., Romby, P., Westhof, E., Ehresmann, C. & Ehresmann, B. (1991) *J. Mol. Biol.* **221**, 293–308.
3. Michel, F. & Westhof, E. (1990) *J. Mol. Biol.* **216**, 585–610.
4. Jaeger, L., Westhof, E. & Michel, F. (1993) *J. Mol. Biol.* **234**, 331–346.
5. Stern, S., Weiser, B. & Noller, H. F. (1988) *J. Mol. Biol.* **204**, 447–481.
6. Westhof, E., Romby, P., Ehresmann, C. & Ehresmann, B. (1990) in *Theoretical Biochemistry and Molecular Biophysics*, eds. Beveridge, D. L. & Lavery, R. (Adenine, New York), pp. 399–409.
7. Altman, S., Kirsebom, L. & Talbot, S. (1993) *FASEB J.* **7**, 7–14.
8. Darr, S. C., Brown, J. W. & Pace, N. R. (1992) *Trends Biochem. Sci.* **17**, 178–182.
9. Brown, J. W. & Pace, N. R. (1992) *Nucleic Acids Res.* **20**, 1451–1456.
10. Burke, J. M., Belfort, M., Cech, T. R., Davies, R. W., Schweyen, R. J., Shub, D. A., Szostak, J. W. & Tabak, H. F. (1987) *Nucleic Acids Res.* **15**, 7217.
11. Massire, C., Gaspin, C. & Westhof, E. (1994) *J. Mol. Graphics*, in press.
12. Jones, T. A. (1978) *J. Appl. Crystallogr.* **11**, 268–278.
13. Westhof, E., Dumas, P. & Moras, D. (1985) *J. Mol. Biol.* **184**, 119–145.
14. Haas, E. S., Morse, D. P., Brown, J. W., Schmidt, F. J. & Pace, N. R. (1991) *Science* **254**, 853–856.
15. Tallsjo, A., Svard, S. G., Kufel, J. & Kirsebom, L. A. (1994) *Nucleic Acids Res.* **21**, 3927–3933.
16. Altman, S., Wesolowski, D. & Puranam, R. (1993) *Genomics* **18**, 418–422.
17. Jaeger, L., Michel, F. & Westhof, E. (1994) *J. Mol. Biol.* **236**, 1271–1276.
18. Shiraishi, H. & Shimura, Y. (1988) *EMBO J.* **7**, 3817–3821.
19. Lumelsky, N. & Altman, S. (1988) *J. Mol. Biol.* **202**, 443–454.
20. Knap, A., Wesolowski, D. & Altman, S. (1990) *Biochimie* **72**, 779–790.
21. Guerrier-Takada, C. & Altman, S. (1993) *Biochemistry* **32**, 7152–7161.
22. Dock-Bregeon, A. C., Westhof, E., Giégé, R. & Moras, D. (1989) *J. Mol. Biol.* **206**, 707–722.
23. Guerrier-Takada, C., Lumelsky, N. & Altman, S. (1989) *Science* **246**, 1578–1584.
24. Burgin, A. B. & Pace, N. R. (1990) *EMBO J.* **9**, 4111–4118.
25. Nolan, J. M., Burke, D. H. & Pace, N. R. (1993) *Science* **261**, 762–765.
26. Mans, R. M. W., Guerrier-Takada, C., Altman, S. & Pleij, C. W. A. (1990) *Nucleic Acids Res.* **18**, 3479–3487.
27. Guerrier-Takada, C. & Altman, S. (1992) *Proc. Natl. Acad. Sci. USA* **89**, 1266–1270.
28. Yuan, Y. & Altman, S. (1994) *Science* **263**, 1269–1273.
29. Kahle, D., Wehmeyer, U. & Krupp, G. (1990) *EMBO J.* **9**, 1929–1937.
30. Rould, M. A., Perona, J. J., Soll, D. & Steitz, T. A. (1989) *Science* **246**, 1135–1142.
31. Dumas, P., Moras, D., Florentz, C., Giegé, R., Verlaan, P., van Belkum, A. & Pleij, C. W. A. (1987) *J. Biomol. Struct. Dyn.* **4**, 707–728.
32. Felden, B., Florentz, C., Giege, R. & Westhof, E. (1993) *J. Mol. Biol.*, in press.
33. Cech, T. R. (1993) in *The RNA World*, eds. Gesteland, R. F. & Atkins, J. F. (Cold Spring Harbor Lab. Press, Plainview, NY), pp. 239–270.
34. Guerrier-Takada, G., Haydock, K., Allen, L. & Altman, S. (1986) *Biochemistry* **25**, 1509–1515.
35. Kazakov, S. & Altman, S. (1991) *Proc. Natl. Acad. Sci. USA* **88**, 9193–9197.
36. Beese, L. S. & Steitz, T. A. (1991) *EMBO J.* **10**, 25–33.
37. Steitz, T. A. & Steitz, J. A. (1993) *Proc. Natl. Acad. Sci. USA* **90**, 6498–6502.
38. Perreault, J.-P. & Altman, S. (1992) *J. Mol. Biol.* **226**, 399–409.
39. Peck, K. A. (1990) Ph.D. thesis (Yale University, New Haven, CT).
40. McClain, W. H. (1977) *Acc. Chem. Res.* **10**, 418–425.
41. Kirsebom, L. & Svärd, S. G. (1993) *Acc. Chem. Res.* **231**, 594–604.
42. Steinberg, S., Misch, A. & Sprinzl, M. (1993) *Nucleic Acids Res.* **21**, 3011–3015.